Available online at www.sciencedirect.com
SCIENCE DIRECT
Biochemical and Biophysical Research Communications 345 (2006) 345–354
BBRC
www.elsevier.com/locate/ybbrc

Characterization of histone (H1B) oxalate binding protein in experimental urolithiasis and bioinformatics approach to study its oxalate interaction

P. Latha [a,*], P. Kalaiselvi [b], P. Varalakshmi [b], G. Rameshkumar [a]

[a] *Department of Life Sciences and Bioinformatics, AU-KBC Research Center, Madras Institute of Technology, Anna University, Chromepet, Chennai 600 044, Tamilnadu, India*

[b] *Department of Medical Biochemistry, Dr. ALM. Post Graduate Institute of Basic Medical Sciences, University of Madras, Taramani Campus, Chennai 600 113, India*

Received 28 March 2006
Available online 27 April 2006

Abstract

The rat kidney H1 oxalate binding protein was isolated and purified. Oxalate binds exclusively with H1B fraction of H1 histone. Oxalate binding activity is inhibited by lysine group modifiers such as 4′,4′-diisothiostilbene-2,2-disulfonic acid (DIDS) and pyridoxal phosphate and reduced in presence of ATP and ADP. RNA has no effect on oxalate binding activity of H1B whereas DNA inhibits oxalate binding activity. Equilibrium dialysis method showed that H1B oxalate binding protein has two binding sites for oxalate, one with high affinity, other with low affinity. Histone H1B was modeled in silico using Modeller8v1 software tool since experimental structure is not available. In silico interaction studies predict that histone H1B-oxalate interaction take place through lysine121, lysine139, and leucine68. H1B oxalate binding protein is found to be a promoter of calcium oxalate crystal (CaOx) growth. A 10% increase in the promoting activity is observed in hyperoxaluric rat kidney H1B. Interaction of H1B oxalate binding protein with CaOx crystals favors the formation of intertwined calcium oxalate dehydrate (COD) crystals as studied by light microscopy. Intertwined COD crystals and aggregates of COD crystals were more pronounced in the presence of hyperoxalauric H1B.

Keywords: Calcium oxalate crystals; Hyperoxaluria; Histone H1B; Oxalate binding protein; Seed crystals; PDB; 2FE2

Calcium oxalate (CaOx) stone disease causes a major health care burden for the human population causing significant pain, morbidity, and hospitalization. Although it is a very common health problem among adults, it is poorly understood at the molecular level, because supersaturation cannot solely explain lithogenesis. Oxalate induced changes in gene expression is now thought to direct the pathogenic events. Two-third of oxalate binding activity of rat kidney and liver homogenate is localized in the nucleus while one-third exists in the mitochondria [1]. Increased oxalate accumulation inside the nucleus against the concentration gradient and its effect on gene expression can be mediated by proteins that have dual binding activity. This suggests that it can bind both oxalate and DNA. H1 histone has been shown to bind oxalate [2]. But the knowledge of the histone fraction that particularly binds oxalate and its role on CaOx crystallization events is vague. Supersaturation, nucleation, aggregation, crystal growth, and retention are the possible sequel of events that leads to stone formation. Retention is one of the important events in etiology of stone formation. Oxalate binding protein which plays a vital role in binding as well as transport of oxalate is implicated in retention as evidenced by mitochondrial oxalate binding protein (62 kDa) which consists of mainly basic amino acids. This protein accumulates oxalate on incorporation into liposomes [3]. Hence, the present study was focused to isolate the fraction of histone that has oxalate

* Corresponding author. Fax: +91 44 222 3 1034.
E-mail address: lathapraba@yahoo.co.in (P. Latha).

0006-291X/$ - see front matter © 2006 Elsevier Inc. All rights reserved.
doi:10.1016/j.bbrc.2006.04.086

binding activity and to evaluate its effect on CaOx crystallization events.

Materials and methods

Adult male Wistar rats weighing 150 ± 20 g were purchased from TamilNadu Veterinary University, Chennai. The animals were maintained under the standard conditions of humidity, temperature (25 ± 2 °C), and light (12 h light/12 h dark). They were fed standard rat pelleted diet (M/s Pranav Agro Industies Ltd., India) under the trade name Amrut rat/mice feed and had free access to water. Experimental animals were handled according to the University and Institutional legislation, regulated by the Committee for the Purpose of Control and Supervision of Experiments on Animals (CPC-SEA), Ministry of Social Justice and Empowerment, Government of India.

Experimental protocol. Animals were randomly divided into two groups. Group I animals served as control. Group II animals served as experimental hyperoxaluric and animals were given 0.75% ethylene glycol for 28 days. All the animals had free access to normal rat chow and water.

Isolation of nuclei. Kidney tissue was excised from the animals following decapitation and quickly dropped into ice-cold saline. A ten percent homogenate of the tissue was made in 0.01 M Tris–HCl containing 0.25 M sucrose, pH 7.4. Nucleus was isolated and purified [4]. Purity was checked by assaying the activities of succinate dehydrogenase and glucose-6-phosphatase for the contamination of mitochondria and microsomes, respectively.

Acid extraction of histone. Nuclear histone was extracted in 0.02 M H_2SO_4 of 0.05 M $NaHSO_3$, precipitated with 95% ethanol [5] and solubilized in 0.2 M acetate buffer, pH 4.5. The protein was estimated by the method of Lowry et al. [6].

Isolation of histone H1. Histone H1 was isolated by the method of Halmer and Gruss [7]. The purified nuclei were incubated with 10 mM triethanolamine, pH 7.0, containing 350 mM NaCl for 15 min on ice. It was then centrifuged at 10,000*g* for 10 min. The pellet was extracted twice with 5% perchloric acid and centrifuged at 10,000*g* for 10 min. Acidified acetone (35 ml acetone and 28.5 μl of 11.6 M HCl) was added to the supernatants and centrifuged at 3000*g* at 15 min. The pellet containing histone H1 was then washed with acetone thrice and was dissolved in distilled water.

Purification and sub-fractionation of histone-oxalate binding protein. About 0.25 mg of perchloric acid extracted histone H1 in 0.5 ml of acetate buffer (0.2 M, pH 4.5) was incubated with [^{14}C]oxalate (50,000 cpm) at room temperature for 20 min. An aliquot was filtered through the 0.45 μm Millipore membrane filter, and the bound oxalate on the filter was measured. [^{14}C]Oxalate bound H1B was further sub-fractionated on CM-cellulose chromatography [8]. Three major peaks were obtained.

The oxalate binding activity of total histone and H1B was assayed using the method of Seethalakshmi et al. [1]. An aliquot of protein (100 μg) was incubated in 1.0 ml of 0.2 M acetate buffer containing 100 nmol/L [^{14}C]oxalate (148 mBq/mmol, Bhabha Atomic Research Center, Trombay, India) at room temperature for 20 min. Non-specific binding was determined in the presence of 100 μM/L unlabeled oxalate. The incubation mixture was filtered through 0.45 μm membrane filters under constant vacuum and the filter was washed twice with acetate buffer. The filters were placed in mini vials and the ^{14}C-oxalate was measured using a liquid scintillation counter.

Equilibrium dialysis studies. One hundred micrograms of protein in 1 ml of 0.2 M phosphate buffer (pH 7.4) containing 0.6% NaCl was taken in one-half of the cell which was segregated by Spectra Por membrane (MWCO 6–8 kDa) from the other half that was filled with 1 ml of [^{14}C]oxalate of different concentrations (500–50,000 cpm) in above buffer. The cell was rotated at 20 rpm for 3 h to reach equilibrium. Aliquots were taken from each compartment and the [^{14}C]oxalate distribution was measured. The oxalate bound to protein was determined by subtracting the free oxalate from total (free + bound). Scatchard plot was plotted using bound (pmol/mg protein) as *x*-axis and bound/free (B/F) in the *y*-axis, from which the dissociation constant ($K_d = 1$/slope) was computed [9].

Crystal growth assay. Crystal growth assay was carried out using the modified method of Fellstrom et al. [10]. Metastable calcium oxalate solutions were prepared by combining the freshly prepared 1.0 ml $CaCl_2$ (3.4 mM) with 1.0 ml of sodium oxalate (0.22 mM) in barbituric acid buffer containing 133 mM NaCl, 0.03% acetic acid, pH 5.7, prepared in deionized water. [^{14}C]Oxalate (50,000 cpm) was added and the metastable solution was allowed to equilibrate for 30 min. Twenty microliters of seed crystal slurry (1.5 mg/ml) was added to the incubation medium. Samples were withdrawn from the chamber prior to the addition of seed crystals at 10 min interval for 40 min, centrifuged, and the aliquot counted in a liquid scintillation counter. The rate of the crystal growth was calculated by the percent loss of [^{14}C]oxalate radioactivity in the filtrate at various time intervals.

Light microscopic studies. Calcium oxalate crystals for light microscopic studies were prepared according to the method of Nakai et al. [11]. Calcium oxalate crystals were formed at room temperature (37 °C) by mixing 20 mM $CaCl_2$ with 20 mM sodium oxalate and 7.6 mM sodium citrate. All the solutions were prepared in 10 mM sodium acetate containing 200 mM sodium chloride. Each solution was adjusted to pH 6.5. Crystallization was carried with or without 10 μg of the respective protein and incubated for 10 min. An aliquot was taken and seen through light microscope.

Modeling of histone H1B molecule. Since the sequence of Wistar rat histone H1B molecule is not available, the sequence of human histone H1B molecule is taken for building the theoretical model. The sequence of Histone H1B molecule is obtained from Swiss-Prot protein database. Swiss-Prot id for this protein is P16401, Gene name of this molecule in Swiss-Prot entry is HIST 1 H1B and chromosomal location is 6p21.3–p22.3. The total length of the nucleotide sequence is 790 bp and the coding region is in between 53 and 733 bp. (http://www.ebi.uniprot.org/entry/P16401). The protein was modeled using the template known as Lyme Disease Variable Surface Antigen VlsE of *Borrelia burgdorferi* having PDBId **1l8w**. Approximately the H1B showed 25% identity and 32% similarity to the template sequence 1l8w. The sequence was manually aligned to increase the similarity and "Iterative Search" method of the MODELLER 8v1 [12] was carried out to get the good model. The predicted model was energy minimized by CHARMM energy minimization.

The predicted model was evaluated using Whatif Web Interface. (http://swift.cmbi.kun.nl/WIWWWI/). The model structure was viewed using Yasara molecular visualization tool [13].

Interaction of H1B molecule with oxalate. Interaction of histone H1B molecule with oxalate was carried out in MEDock server [14]. The MEDock web server incorporates a global search strategy that exploits the maximum entropy property of the Gaussian probability distribution in the context of information theory. As a result of the global search strategy, the optimization algorithm incorporated in MEDock is significantly superior when dealing with very rugged energy landscapes, which usually have insurmountable barriers (http://medock.csie.ntu.edu.tw/).

The experimental setup for running the docking is given in tabular form.

Docking runs	5
Generation time	1000
Grid spacing	0.375
Local search	0.05
Population size	50
Random seed time	—

The hydrogen bonding and hydrophobic contacts between H1B and oxalate was identified using "LIGPLOT v 4.4.2 tool." This program automatically generates a schematic diagram of protein–ligand interactions for a given PDB file [15].

Statistical analysis. Statistical analysis was carried out with Student's *t* test. Data are presented as means ± SD.

Results

Oxalate binding activity of total histone and oxalate binding activity of kidney H1B is shown in Tables 1 and 2 respectively. Oxalate binding activity was determined

Table 1
Oxalate binding activity of total histone

Particulars	Acetate buffer (pmol bound/mg protein)	Phosphate buffer (pmol bound/mg protein)
Kidney	20.8 ± 1.8	8.6 ± 1.0

Values are expressed as means ± SD for six experiments.
One hundred micrograms histone was incubated with 0.2 M acetate buffer (pH 4.5)/0.05 M phosphate buffer (pH 7.4). The oxalate binding activity was carried out as described in Materials and methods.

Table 2
Oxalate binding activity of control and hyperoxaluric histone H1B

Particulars	Oxalate binding activity (pmol bound/mg protein)	
	Control	Hyperoxaluria
0.2 M acetate buffer		
Kidney H1B	200.8 ± 17.8	262.2 ± 18.4*
0.05 M phosphate buffer		
Kidney H1B	29.6 ± 4.3	43.3 ± 4.8*

Values are expressed as means ± SD for six experiments.
One hundred micrograms H1 was incubated with 0.2 M acetate buffer (pH 4.5) and 0.05 M phosphate buffer (pH 7.4). The oxalate binding activity was carried out as described in Materials and methods.
* $p < 0.001$.

for both control and hyperoxaluric histone-H1B at pH 4.5 (acetate buffer) and pH 7.4 (phosphate buffer). The oxalate binding activity was higher at pH 4.5 than at pH 7.4. Oxalate binding activity for total histone derived from control kidney was 20.8 pmol of oxalate bound/mg protein whereas for the kidney histone-H1B it was 200.8 pmol - bound/mg protein. Oxalate binding activity of H1B was 10-fold higher than crude histone. Oxalate binding activity was significantly higher for hyperoxaluric H1B oxalate binding protein when compared to control ($p < 0.001$).

Purification profile of histone H1B oxalate binding protein

The histone H1 protein isolated by single step purification method was further sub-fractionated on Carboxymethyl-Sephadex C-50 ion exchange column chromatography. Three protein peaks were obtained in the order of H1B, H1A, and $H1^0$ (Fig. 1a and Table 3). The radioactive peak was exclusively associated with H1B fraction. The yield of the control H1B protein was 34% with specific activity of 5.5 pmol/μg protein. The protein was 1.47-fold purified. The yield of hyperoxaluric H1B protein was 40% with specific activity of 6.5 pmol/μg protein. The protein was 1.5-fold purified (Fig. 1b and Table 3).

Table 4 depicts total histone content and H1 content in kidney. The amount of total histone present in the kidney was found to be 1.5 mg/g tissue; H1 isolated by single step purification method was 80 μg/g tissue. H1 content was found to be increased in hyperoxaluric kidney. The percentage stimulation of protein content was around 9%. The percentage stimulation for oxalate binding activity for hyperoxaluric kidney H1 was approximately 30%.

Kinetic studies on H1B oxalate binding protein

The optimum temperature for [^{14}C]oxalate binding to histone-H1B was at 30 °C for both control and EG treated rats. No further increase in activity was detected at other temperature (data not shown). Oxalate binding to histone-H1B was found to be optimum at 100 μg concentration for both control and hyperoxaluric animals (data not shown).

Lysine group modifiers such as (DIDS) and pyridoxal phosphate showed concentration-dependent inhibition on oxalate binding. Fifty percent reduction of oxalate binding activity was noted at 10 μM concentration of DIDS. At 10 mM concentration of DIDS, the oxalate binding activity was completely abolished (Table 5) whereas the oxalate binding activity of H1B was completely abolished at the concentration of 1 mM pyridoxal phosphate.

DNA or RNA as such had no oxalate binding activity. However, when DNA was pre-incubated with kidney histone H1B, the oxalate binding activity was significantly reduced ($p < 0.001$). RNA had no effect on oxalate binding activity of histone H1B (Table 6).

Pre-incubation of kidney histone-H1B with nucleotides such as ADP and ATP significantly reduced the oxalate binding activity ($p < 0.001$). At 1 mM ATP concentration, oxalate binding was completely abolished (Fig. 2) but AMP had no effect on oxalate binding activity of H1B.

Scatchard plot analysis revealed the presence of two binding sites, the high affinity site with dissociation constant (K_d) of 32 nM and maximal binding capacity (B_{max}) 42 pmol of oxalate/mg protein and another one with low affinity site, having a dissociation constant (K_d) of 428 nM and B_{max} 170 pmol of oxalate/mg protein for control kidney histone H1B oxalate binding protein (Fig. 3a) and hyperoxaluric kidney histone H1B also showed the presence of two affinity sites, high affinity site with dissociation constant (K_d) of 214 nM and maximal binding capacity (B_{max}) 84 pmol of oxalate/mg protein and a low affinity site, with dissociation constant (K_d) of 797 nM and (B_{max}) 252 pmol of oxalate/mg protein (Fig. 3b).

Effect of H1B oxalate binding protein on in vitro CaOx crystals

Crystal growth attained equilibrium by 40 min. The control kidney H1B protein promoted crystal growth by 21% at the concentration of 10 μg whereas hyperoxaluric kidney histone H1B promoted crystal growth by 32%, at the same concentration. Approximately 10% increase in promoting activity was observed for hyperoxaluric rat kidney H1B (Fig. 4).

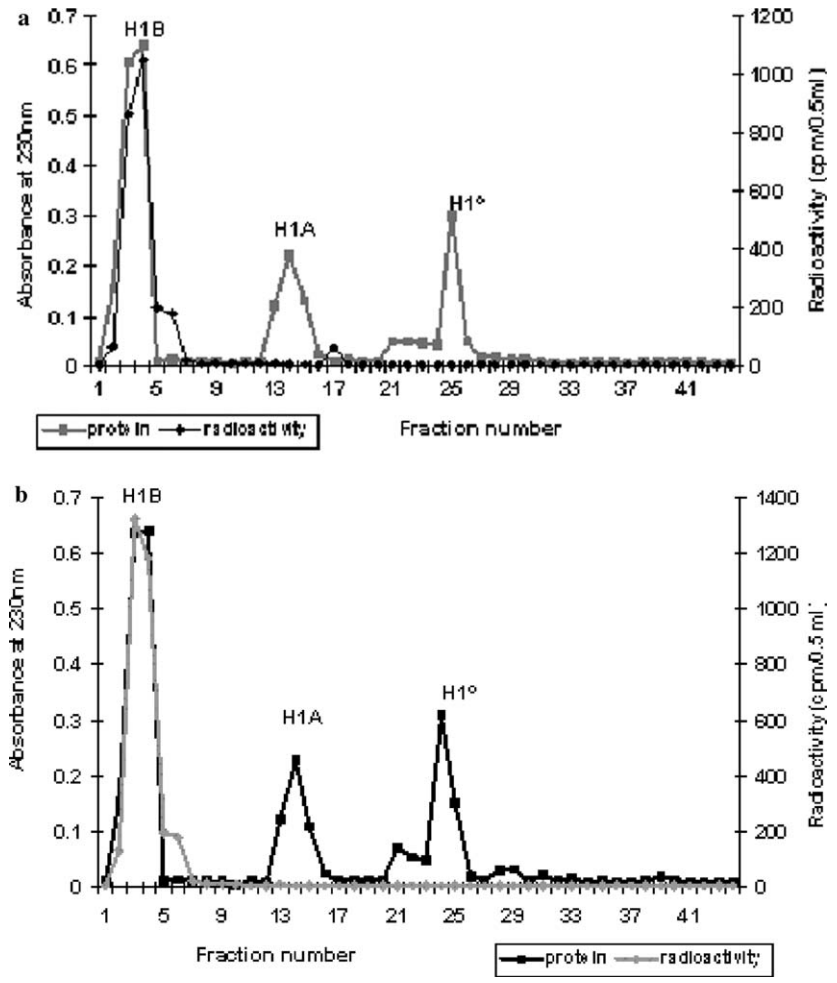

Fig. 1. (a) CM-Sephadex elution profile of control kidney histone H1B. (b) CM-Sephadex elution profile of hyperoxaluric kidney histone H1B.

Table 3
Purification profile of control renal H1B on CM-Sephadex Column Chromatography

Particulars	Volume of fraction (ml)	Total protein (μg)	Total oxalate bound (pmol)	Specific activity (pmol/μg protein)	Yield %	Fold purification
Control						
PCA extracted H1	0.5	250	933	3.72	100	1
CM-Sephadex subfractionated H1B	15	85	468	5.5	34	1.47
Hyperoxaluria						
PCA extracted H1	0.5	250	1091	4.364	100	1
CM-Sephadex subfractionated H1B	15	100	650	6.5	40	1.5

Control and hyperoxaluric kidney histone-H1 were incubated with [^{14}C]oxalate (50,000 cpm). Aliquot of 0.1 ml was filtered through 0.45 μm (Milipore) membrane filter and the filter was washed twice with 0.2 M acetate buffer, pH 4.5 and the radioactivity retained by the filter was measured as described in Materials and methods. The sample was loaded and the elution was carried out as described in Materials and methods.

Light microscopic studies

Fig. 5 depicts representative microscopic field of 400× magnification. Fig. 5a represents only COD crystals formation without any additives. Intertwined COD crystals were formed in the presence of control kidney H1B (Fig. 5b and c) while intertwined COD crystals and aggregates of COD crystals were prominent in the presence of hyperoxaluric kidney H1B (Fig. 5d and e).

Theoretical modeling of histone H1B

In order to study the interaction of H1B molecule with oxalate in in silico, homology modeling of this protein on MODELLER8v1 was carried out. Since the complete sequence of wistar rat H1B is not available, human H1B was taken as query. The MODELLER8v1 software referred five best template sequences from inbuilt template database library of its own. The best template was chosen based on

Table 4
Histone H1 content and its [^{14}C]oxalate binding activity in rat kidney

Particulars	Total histone protein (μg/g tissue)	Oxalate binding activity (pmol bound/mg protein)	H1-histone protein (μg/g tissue)	Oxalate binding activity (pmol bound/mg protein)
Control kidney	1598.08 ± 105.22	16.7 ± 2.4	80.1 ± 3.8	200.4 ± 21.1
Hyperoxaluric kidney	1720.21 ± 102.14*	22.1 ± 1.8***	87.2 ± 3.6**	260.1 ± 20.9***

Values are expressed as means ± SD for six experiments. Protein content as well as oxalate binding activity was measured as described in Materials and methods. Values are statistically significant when compared with control.
* $p < 0.05$.
** $p < 0.01$.
*** $p < 0.001$.

Table 5
Effect of lysine group modifiers (DIDS and pyridoxal phosphate) on kidney H1B oxalate binding activity

Particulars	Control	Oxalate binding activity (pmol bound/mg protein)				
		1 μM	10 μM	100 μM	1 mM	10 mM
DIDS	198.8 ± 19.8	121 ± 11.8	92.8 ± 8.1*	35.8 ± 6.8*	18.4 ± 2.6*	—
Pyridoxal phosphate	193.8 ± 18.9	98.8 ± 9.7*	49.4 ± 8.5*	28.6 ± 6.5*	—	—

Values are expressed as means ± SD for six experiments. Lysine group modifiers such as DIDS and pyridoxal phosphate were incubated in different concentration with the H1B protein and oxalate binding activity was carried out as described in Materials and methods. Values are statistically significant when compared to control having no modifiers.
* $p < 0.001$.

Table 6
Effect of DNA and RNA on oxalate binding activity of histone H1B

Particulars	Oxalate binding (pmol bound/mg protein)
Kidney histone H1B	194.6 ± 11.4
DNA	—
Kidney histone H1B + DNA	50.4 ± 8.3*
RNA	—
Kidney histone H1B + RNA	198.4 ± 9.6

Values are expressed as means ± SD for six experiments. Oxalate binding activity was carried out in the presence of DNA and RNA as described in Materials and methods. Values are statistically significant when compared to their respective histone oxalate binding activity.
* $p < 0.001$.

the similarity and expectation value. Although the molecule with PDBId '**1ust**' (NMR structure of yeast histone H1 globular domain I) and "**1ghc**" (NMR structure of *Gallus gallus* HISTONE H1 GLOBULAR DOMAIN I) showed good similarity (above 85%) with the histone H1B but for the partial sequence of H1B sequence. Hence, both the sequences were omitted for using as template. This template PDBId '**1l8w**' protein showed 32% similarity to histone H1B molecule up to the entire length of the sequence. X-ray crystal structure of **1l8w** (Crystal Structure of Lyme Disease Variable Surface Antigen VlsE of *B. burgdorferi*) is available in PDB with the resolution factor of 2.6. The template coordinate files are then downloaded from protein Data Bank (PDB). The model was built and the inbuilt DOPE (Discrete optimized Energy) score of this modeled protein is −2.299 kJ/mol. DOPE Score is a statistical potential optimized for model assessment, to assess the quality of model. The model was evaluated in Whatif web interface which indicates that *Z* score and Ramachandran plot values are found to be good. The model was deposited in PDB using **AutoDep** tool and assigned a PDB Id 2FE2 for this theoretically modeled protein. The structure of 2FE2 was visualized in Yasara molecular visualization software tool (Fig. 6a and b). 2FE2 structure contains 11 helices (54.7%), two strands (2.2%), 23 turns (17.3%), and 25.8% coils.

Interaction of 2FE2 with oxalate molecule

MEDock server results suggest that three amino acid residues are involved in interaction with oxalate molecule. Reproducibility of the result is excellent with this server. LYS121, LYS 213, and LEU68 are involved in interaction with oxalate with the lowest docked energy of −4.1352 kcal/mol. The hydrogen bond distance between ε-amino group of LYS121 and O3 (third oxygen) of oxalate molecule is 2.67, the hydrogen bond distance between ε-amino group of LYS139 and O4 (fourth oxygen) of oxalate molecule is 3.15 and the hydrogen bond distance between α-nitrogen of LEU68 and O2 (second oxygen) of oxalate molecule is 2.95 which indicates that two side chain molecule of lysine residues and one α-nitrogen group of leucine is involved (Fig. 7). This study characterizes the one oxalate binding site which involves three amino acid residues. The other binding site which is involved in interaction with oxalate molecule should be explored further.

Discussion

Oxalate binding protein plays a vital role in binding as well as transport of oxalate in the cell. Several oxalate binding proteins have been identified in our laboratory

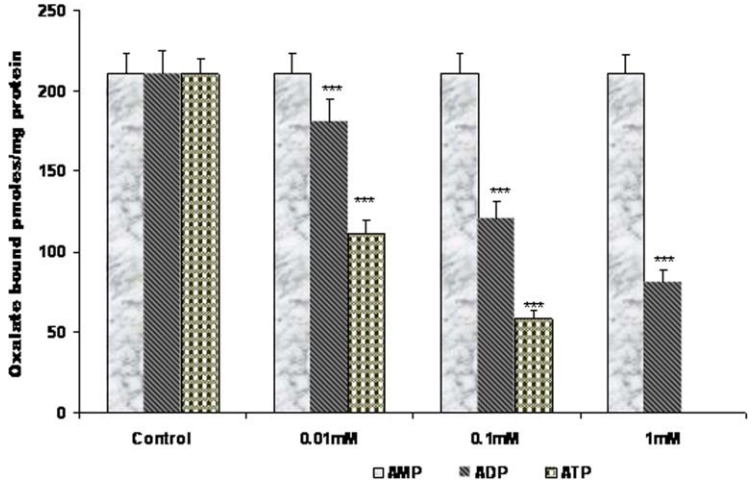

Fig. 2. Oxalate binding activity of control kidney H1B on addition of nucleotides. Various concentrations of nucleotides such as AMP, ADP, and ATP were incubated with kidney histone H1B and oxalate binding activity was measured as described in Materials and methods. ADP and ATP inhibited oxalate binding activity while AMP had no effect on oxalate binding activity of kidney histone H1B. Values are means ± SD for six experiments. Values are statistically significant when compared with control having no nucleotides. ***$p < 0.001$.

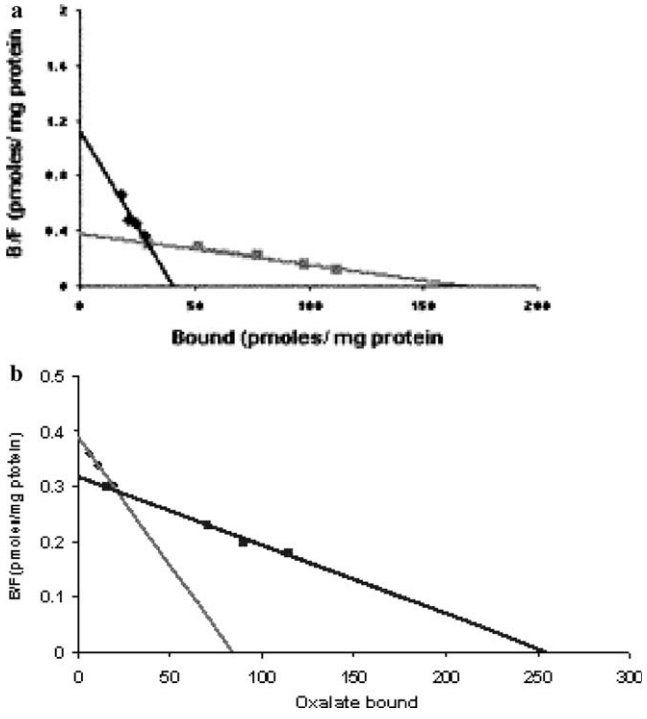

Fig. 3. Various concentrations of oxalate on oxalate binding activity of histone H1B. Scatchard plot characterizes relationship between concentration of oxalate and its binding. Purified control (a) and hyperoxaluric kidney histone H1B (b) were incubated with various concentrations of [^{14}C]oxalate (500–50,000 cpm). Oxalate binding was measured by equilibrium dialysis method as described in Materials and methods.

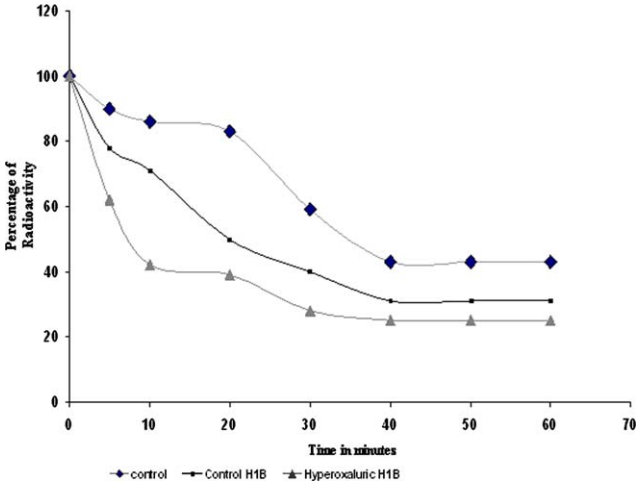

Fig. 4. The effect of histone H1B on CaOx crystal growth was studied as described in Materials and methods. Control kidney H1B was found to have promoting effect on CaOx crystal growth. Increase in promoting activity (10%) was noted for hyperoxaluric kidney histone H1B. Values are means ± SD for six experiments.

including nuclear oxalate binding histone H1 from rat and human kidney [2], calcium oxalate binding protein [16], and nuclear pore complex oxalate binding protein [17]. In our early studies we have shown that nuclear oxalate binding activity is distributed between histone H1B and nuclear pore complex protein gp210. The physiological significance of this histone H1B protein in stone formation is ambiguous. H1 isolated by the previous methods are time consuming and the yield is very less. The present study involves a single step purification method. The oxalate binding to H1B is concentration, temperature, and pH dependent. Increased oxalate binding activity in acidic pH is physiologically significant, because the nucleus is slightly acidic than the cytosol. This protein is also found to be very stable and oxalate binding seems to be very specific. Oxalate binding activity was higher with H1B (200.8 pmol/mg protein) when compared to total histone (20.8 pmol/mg protein).

The enhanced oxalate binding activity has been observed in hyperoxaluric kidney H1B. Increased oxalate binding

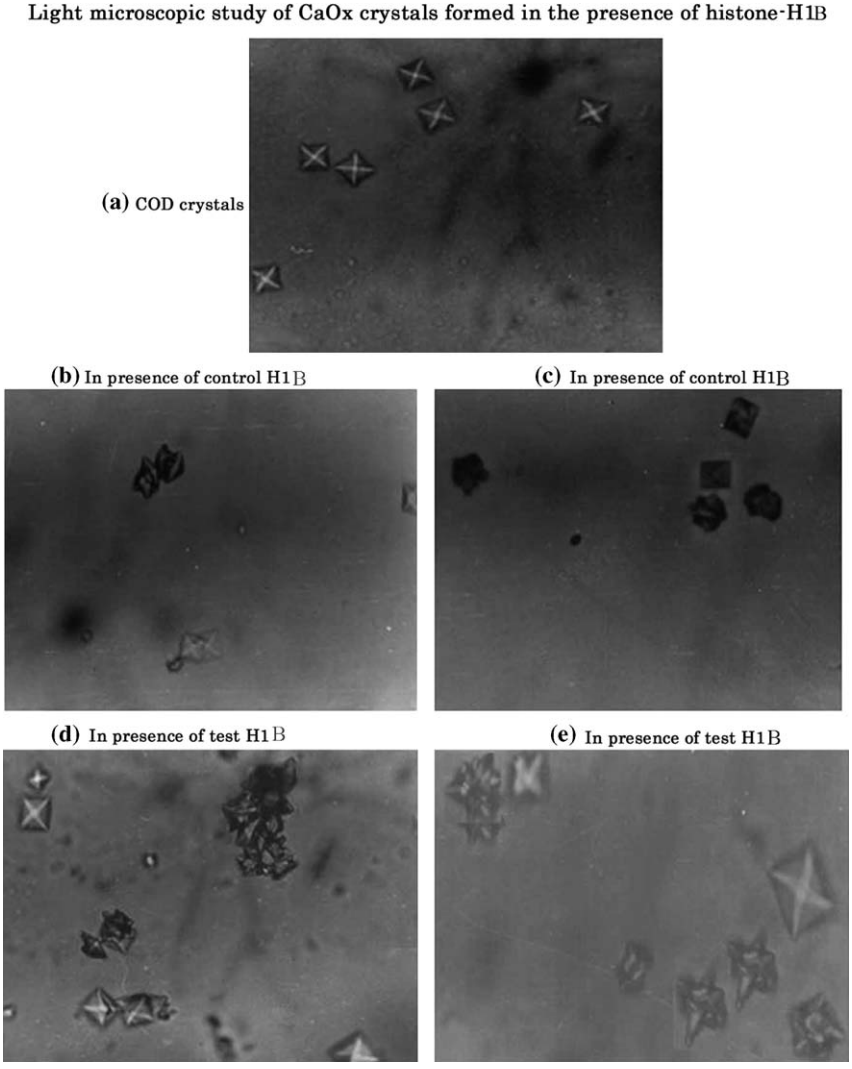

Fig. 5. (a) CaOx crystals in the absence of histone H1B. (b,c) CaOx crystals in the presence of control H1B. (d,e) CaOx crystals in the presence of hyperoxaluric H1B.

activity observed during hyperoxaluria, might be due to the oxalate induced modification of protein. Oxidative stress mediated modification of protein and increased oxalate binding activity have already been encountered for stone matrix protein [18] and calcium oxalate binding protein [19]. Oxalate is shown to reduce the redox status of the cell as evidenced by the reduced antioxidant status in hyperoxaluric model [20]. Enhanced formation of H1B of histone H1 in rats fed with diet low in methionine and cysteine was observed [21]. Kannabiran and Selvam [2] have already shown that the increased histone expression occurs during hyperoxaluria. Increased histone expression may be deleterious to the cells because they might be involved in the retention of CaOx crystals since they bind more oxalate and promote nucleation and aggregation of CaOx.

The optimum pH for oxalate binding to histone H1B protein is found to be 4.2 with 0.2 M sodium acetate buffer. This acidic pH is necessary to maintain the protein in its soluble form with maximum activity. pH plays an important role for oxalate uptake in rat colon with a maximum activity at pH 6.8 [22]. Among the three major CaOx binding proteins isolated from human kidney, two proteins (FI and FII) have high activity at pH 7.4, while the FII has optimum oxalate binding activity at pH 4.5 [23].

Lysine group modifiers such as DIDS and pyridoxal phosphate are found to inhibit the oxalate binding activity completely, suggesting that lysine group of histone-H1 is involved in oxalate binding. Similarly, anion transport band 3 protein is also inhibited by DIDS which is shown to bind to the proximal and distal lysine ε-amino group present in or near the external opening [24].

Nucleotides such as ATP and ADP inhibit oxalate binding of histones-H1B, while AMP has no effect on oxalate binding. Histone-H1 is capable of recognizing nucleoside tri phosphates (NTPs) and nucleoside diphosphates (NDPs) such as ATP, GTP, ADP, and GDP [25]. Several nucleotide binding motifs have been identified in histone protein. A Gly-X-Gly-X-X-Gly phosphate binding motif is common to the majority of nucleotide binding proteins [25] and is present in globular region of histone-H1. The

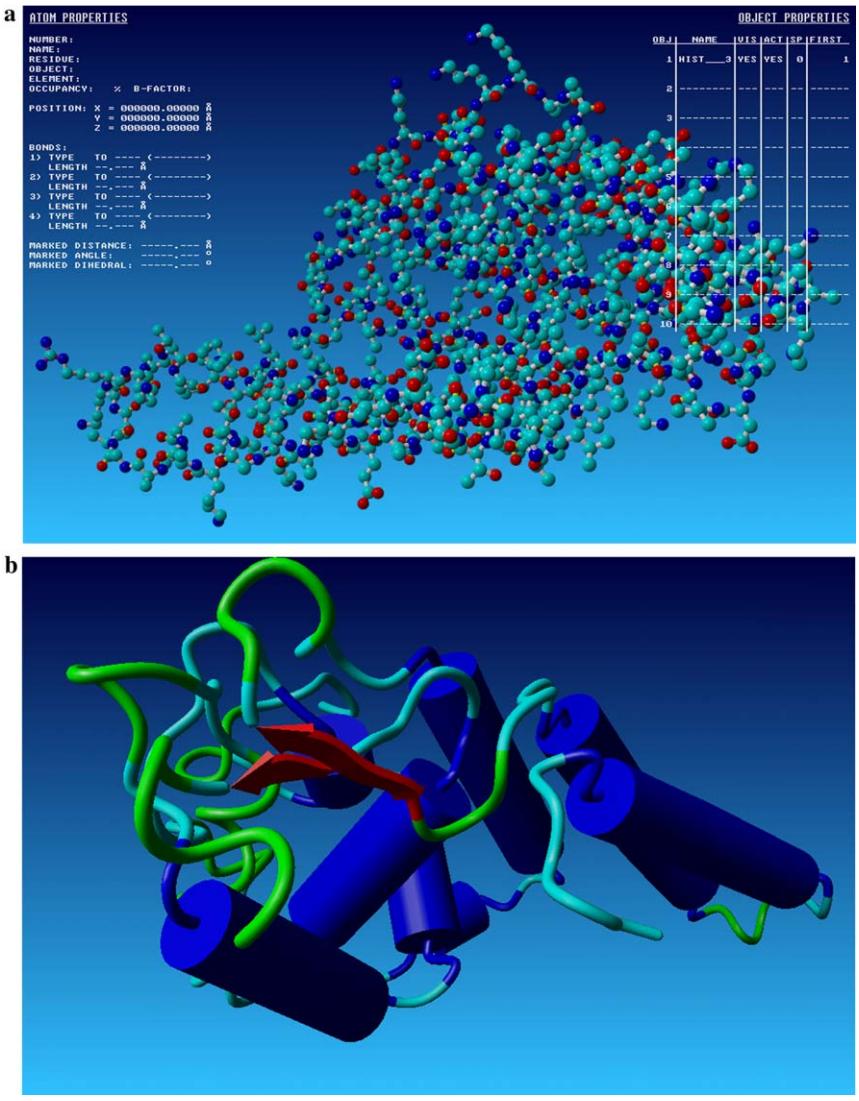

Fig. 6. (a) Ball and stick model of 2FE2 seen by YASARA molecular visualization software tool. The blue color represents nitrogen atom, red color represents oxygen atom, and light blue represents carbon atoms. The yellow color represents double bond between main chain carbon and oxygen. The white color bond represents single bond between carbon and nitrogen. (b) Secondary structure representation of 2FE2. The blue color bundle depicts α-helices and red color arrow depicts strands. (For interpretation of the references to colour in this figure legend, the reader is referred to the web version of this paper.)

reduced oxalate binding activity observed in the presence of nucleotide suggests that the nucleotides might provide steric hindrance for the binding of oxalate.

DNA and RNA have no oxalate binding activity; however histone-H1B oxalate binding activity is reduced in the presence of DNA, while RNA has no effect on oxalate binding activity. Reduction of oxalate binding to H1B in presence of DNA suggests that DNA affects the binding activity of oxalate. Histone-H1 binds to DNA at specific A + T rich regions, the interaction taking place through SPKK motifs in its tail [26]. When nucleotides or DNA bind to these sites, probably a distortion is induced in the oxalate binding site. Either pre-incubation or post-incubation with DNA affects oxalate binding activity, suggesting the greater affinity of histones to DNA rather than oxalate.

Scatchard plot analysis shows the presence of low and high affinity sites in both control and hyperoxaluric histone-H1B. The affinity for oxalate is reduced for the H1B derived from hyperoxalauric kidneys. Even though the affinity is reduced, B_{max} of the test H1B is increased, suggesting that it could hold more oxalate than the control H1B. During hyperoxaluria, since the in vivo oxalate concentration increases, it might favor the retention of oxalate because H1B has affinity towards CaOx crystals.

Computational analysis of theoretical modeling of histone H1B (2FE2) and its interaction with oxalate molecule is the novel idea to confirm the affinity of lysine residues to oxalate molecules. Further these lysine residues can be mutated to see how this interaction is modified. This is yet to be an important milestone in interaction studies which is to be explored further. In silico toxicity analysis of oxalate is also a future plan.

In seeded crystal system, kidney H1B promotes CaOx crystal growth. There is 10% increase in promoting

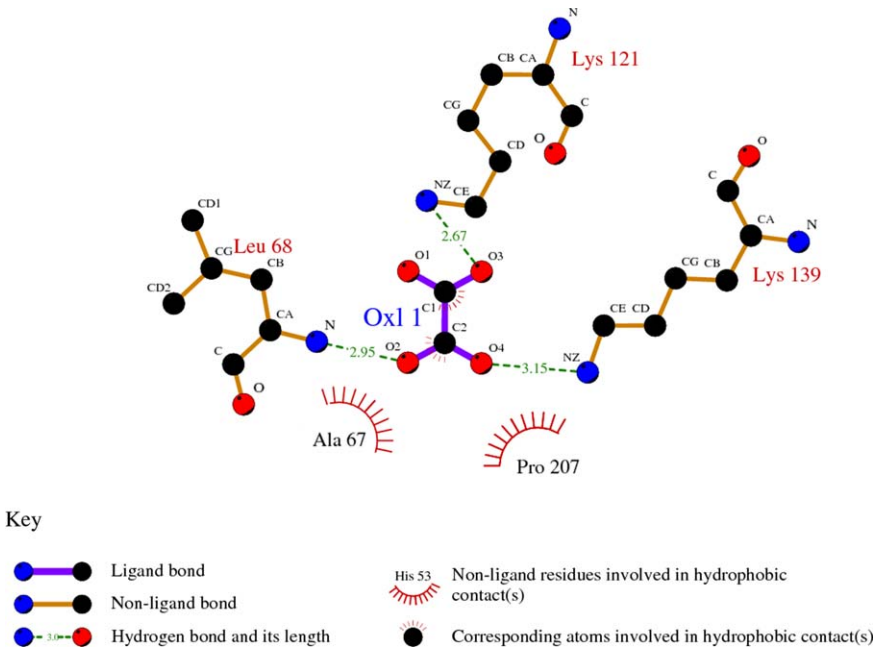

Fig. 7. Ligplot representation of 2FE2 with oxalate interaction. Oxalate is present in the center of the view. Hydrogen bonds are indicated by dashed lines between the atoms involved and hydrophobic contacts are represented by an arc with spokes radiating towards the ligand atoms. Lys121, Lys139, and Leu68 are involved in hydrogen bond interaction while Ala67 and Pro207 are involved in hydrophobic contacts.

activity observed in hyperoxaluric rat kidney when compared to control. Kidney H1B has also been shown to promote nucleation and aggregation (data not shown) of CaOx crystals. Pure promoters of stone formation are rare. A urinary 45 kDa protein isolated in our laboratory is found to be an inhibitor of nucleation and aggregation, whereas the same protein in hyperoxaluric condition acts as promoter of nucleation and weak inhibitor of aggregation [19]. COM binding protein (45 kDa) which is found to promote CaOx crystallization constitutes mainly basic amino acids [3]. Stone formers Tom–Horsfall glycoprotein (THP) and nitrosylated-THP have been shown to promote CaOx nucleation and aggregation whereas THP derived from healthy subject's urine was found to be an inhibitor [27]. Stone matrix protein (48 kDa) is found to be a promoter of crystal growth as well as nucleation and aggregation of CaOx crystals [18]. Interaction of H1B histone with CaOx crystals favors the formation of intertwined COD crystals. A 23 kDa-calcium oxalate monohydrate (COM) binding protein derived from control urine favors the formation of COM crystals and intertwined COD crystals [28]. Urinary macromolecules appear to cause interpenetration twining of COD crystals because they are widespread in urine and urinary stones. The macromolecules with multiple crystal binding sites can attach to many crystals and bring them closer promoting viscous binding and polymer bridging [29]. Similar mechanism can be involved with histone H1B, since it also has more than one oxalate binding site.

The kidney H1B histone promotes CaOx crystallization and enhanced oxalate binding activity, as observed in hyperoxaluria, this may favor crystal retention. Histones may bind with oxalate moiety of CaOx crystals and attract further crystals which then occlude the tubular lumen. Histone also has preferential binding to the glomerular basement membrane. It is evident that nucleosome/autoantibody complex binds to the glomerular basement membrane via interaction of cationic histone moieties present in the nucleosome to the anion moiety heparan sulfate [30]. Thus it may be possible for the bound histone associated CaOx crystals in the membrane to act as nidi for further crystal growth which might damage the urothelium and injury of urothelial cells further aggravates stone formation.

The modulatory effect of H1B on CaOx crystallization might be the reason for nuclear oxalate retention. The increased promoting activity observed in hyperoxaluric H1B has significance in driving the path of microliths to macroliths during stone formation. To conclude our results, histone (H1B) has oxalate binding activity and its interaction occurs via lysine residues which is confirmed by both in vitro and in silico methods. The high oxalate binding activity occurred in hyperoxaluric condition may be due to significant impact of oxalate on histone H1B. The enhanced oxalate binding activity and CaOx crystallization promoting activity of hyperoxaluric H1B of histone H1 fraction suggest that it may play a crucial role in retention and stone formation in renal cells.

Acknowledgment

Dr. P. Latha was a recipient of Senior Research Fellowship from the Department of Science and Technology, New Delhi.

Appendix A. Supplementary data

Supplementary data associated with this article can be found, in the online version, at doi:10.1016/j.bbrc.2006.04.086.

References

[1] L. Seethalakshmi, R. Selvam, C.J. Mahle, M. Menon, Binding of oxalate to mitochondrial inner membranes of rat and kuman kidney, J. Urol. 135 (1986) 862–865.
[2] R. Selvam, K. Kannabiran, Characterisation of nuclear oxalate binding of rat and human kidney, J. Urol. 156 (1996) 237–242.
[3] R. Selvam, P. Kalaiselvi, Oxalate binding proteins in calcium oxalate nephrolithiasis, Urol. Res. 31 (2003) 242–256.
[4] G. Blobel, V.R. Porter, Nuclei from rat liver: isolation method that combines purity with high yield, Science 154 (1996) 1662–1665.
[5] J. Bonner, G.R. Chalkley, M. Dahmus, D. Fambrough, F. Fujimura, R.C. Huang, J. Huberman, R. Jensen, K. Maruahige, H. Ohlenbausch, B.M. Olivera, J. Widholm, Isolation and characterization of chromosomal nucleoprotein, Methods Enzymol. 12 (1968) 3–5.
[6] O.H. Lowry, N.J. Rosebrough, A.L. Farr, R.J. Randall, Protein measurement with the folin–phenol reagent, J. Biol. Chem. 193 (1951) 265–274.
[7] L. Halmer, C. Gruss, Isolation H1 by single step purification method, Nucleic Acids Res. 23 (1995) 773–778.
[8] T. Banchev, L. Srebeva, J. Zlatanova, Purification of histone $H1^0$ and its subfractions under non denaturing conditions, Biochim. Biophys. Acta 1073 (1991) 230–232.
[9] U.K. Laemmli, Cleavage of structural proteins during the assembly of the head of bacteriophage T4, Nature (Lond.) 227 (1970) 680–685.
[10] B. Fellstrom, Bo.G. Danielson, S. Ljunghall, B. Wikstrom, Crystal inhibition: the effects of polyanions on calcium oxalate crystal growth, Clin. Chim. Acta 158 (1986) 229–235.
[11] H. Nakai, M. Yamagawa, K. Kameda, Y. Ogawa, J. Kawamura, Transformation of calcium oxalate dihydrate crystals in solution: Why is not calcium oxalate dihydrate detected in urinary calculi, Published in: symposium on Urolithiasis, Urolithiasis'96 (1996) 323–325.
[12] M.A. Marti-Renom, A. Stuart, A. Fiser, R. Sánchez, F. Melo, A. Sali, Comparative protein structure modeling of genes and genomes, Annu. Rev. Biophys. Biomol. Struct. 29 (2000) 291–325.
[13] E. Krieger, G. Koraimann, G. Vriend, Increasing the precision of comparative models with YASARA NOVA—a self-parameterizing force field, Proteins 15/4 (3) (2002) 393–402.
[14] D.T. Hau Chang, Y.J. Oyang, J.H. Lin3, MEDock: a web server for efficient prediction of ligand binding sites based on a novel optimization algorithm, Nucleic Acids Res., 33 Web Server Issue (2005) W233–W238.
[15] A.C. Wallace, R.A. Laskowski, J.M. Thornton, LIGPLOT: a program to generate schematic diagrams of protein–ligand interactions, Protein Eng. 8 (1995) 127–134.
[16] M. Adhirai, R. Selvam, Renal calcium oxalate binding protein: studies on its properties, Kidney Int. 53 (1998) 125–129.
[17] R. Selvam, R. Vijaya, P. Sivagamasundari, Characterization of nuclear pore complex oxalate binding protein from human kidney, Mol. Cell. Biochem. 243 (2003) 1–8.
[18] A. Govindaraj, R. Selvam, An oxalate-binding protein with crystal growth promoter activity from human kidney stone matrix, Br. J. Urol. Int. 90 (2002) 336–344.
[19] R. Selvam, S. Balakrishnan, P. Kalaiselvi, Effect of hyperoxaluria on the inhibitory activity of a 45 kDa urinary protein, Nephron 604 (2002) 1–7.
[20] A. Muthukumar, R. Selvam, Effect of depletion of reduced glutathione and its supplementation by glutathione monoester on renal oxalate retention in hyperoxaluria, J. Nutr. Biochem. 8 (2002) 1–6.
[21] M. Norell, A. Von der Decken, Effects of a diet low in methionine–cysteinie on rat liver chromatin and nuclear proteins, Cell. Mol. Biol. 35 (1989) 63–74.
[22] S.E. Schwartz, J.Q. Stauffer, L.W. Burgess, M. Cheney, Oxalate uptake by averted sacs of rat colon- Regional differences and the effects of pH and ricinoleic acid, Biochem. Biophys. Acta 596 (1980) 404–413.
[23] R. Selvam, P. Kalaiselvi, A novel basic protein from human kidney which inhibits calcium oxalate crystal growth, Br. J. Urol. 86 (2000) 7–13.
[24] M. Ramjee Singh, A. Gaarn, A. Rothstein, The location of disulfonic stilbene binding site in band 3, the anion transport protein of the red blood cell membrane, Biochim. Biophys. Acta 599 (1980) 127–139.
[25] R.M. Mannermaa, J. Oikarinen, Nucleoside triphosphate binding and hydrolysis by histone H1, Biochem. Biophys. Res. Commun. 182 (1992) 309–317.
[26] M.E.A. Churchill, M. Suzuki, 'SPKK' motifs prefer to bind to DNA at A/T-rich sites, EMBO J. 8 (1989) 4189–4195.
[27] V. Pragasam, P. Kalaiselvi, B. Subashini, K. Sumitra, P. Varalakshmi, Structural and functional modification of THP on nitration: comparison with stone formers THP, Nephron Physiol. 99 (2005) 28–34.
[28] D. Asokan, P. Kalaiselvi, P. Varalakshmi, Modulatory effect of the 23-kDa calcium oxalate monohydrate binding protein on calcium oxalate stone formation during oxalate stress, Nephron Physiol. 97 (2004) 23–30.
[29] S.R. Khan, Animal models of kidney stone formation: an analysis, World J. Urol. 15 (1997) 236–243.
[30] M.C.J. Van Bruggen, B. Walgreen, T.P. Rijke, W. Tamboer, K. Kramers, R.J. Smeenk, M. Monestier, G.J. Fournie, J.H. Berden, Antigen specificity of anti-nuclear antibodies complexed to nucleosomes determines glomerular basement membrane binding in vivo, Eur. J. Immunol. 27 (1997) 1564–1569.